

# Dry-Type Power Transformers Thermal Analysis with Finite Element Method

Lucas R. Torin, Daniel O. G. Medina, Thales Sousa

Centro de Engenharia, Modelagem e Ciências Sociais Aplicadas, CEP: 09210-580, Santo André/SP, Brazil

Email:

**Abstract**— *The transformer temperature is one of the main variables of interest in its manufacture and operation, since it interferes in the useful life of the transformer. In this sense, the present work proposes a thermal simulation for the temperature estimate of a dry-type transformer. Initially a thermal analysis was performed from experimental measurements of temperatures of a dry-type power transformer of 500kVA for different conditions of load. Posteriorly, a thermal simulation was proposed using finite element theory. Thus, the heat diffusion equation was used, with the following boundary conditions: convection and radiation equations; characteristics of the materials used; the measurement data and the dimensions of the transformer. FEMM 2D software was used for the proposed simulation. Finally, in order to validate the proposed analyzes, experimental measurements were compared with the values obtained in the thermal simulation. The results of the thermal simulation showed agreement with the experimentally measured values.*

**Keywords**— *Dry-type transformers, Experimental measurement, Finite elements, Thermal simulation.*

## I. INTRODUCTION

Dry-type transformers are widely used in electric power distribution systems and are recommended for smaller indoor installations that require safety and reliability, require less maintenance and less damage to the environment [1].

The design and overload capacity of transformers are strongly influenced by thermal performance and behavior. The thermal influence on the power transformers is very relevant, and one of the main interest factors in the operation of transformers is the temperature, since it interferes with the aging of the insulation of the winding and, consequently, its useful life. Therefore, the temperature monitoring is essential to evaluate, in general, the wear of the transformer [2].

Studies have shown that the temperature is one of the major causes of deterioration of insulation material of power transformers and thermal stress. This thermal stress, caused by heat, is a condition where the insulation

material is affected by the temperature of the environment in which it is located, when this temperature is at extreme levels, and which has resulted in electrical faults in the distribution systems. A temperature distribution and overload or overheating is a particular interest of manufacturers and customers with the purpose of prolonging the life expectancy of transformers [3], [4].

Also, in the design stage, in order to estimate the temperature, there are several numerical methods of thermal simulation, capable of dealing with complex geometries and that become important tools for the transformer designer. In this sense the finite element method (FEM) comes being widely applied after the evolution of the computational systems [5].

Considering FEM this work presents an analysis through the simulation of the results of theoretical and experimental investigations of the thermal behavior of a dry-type power transformer, when this is subject to different load conditions.

These investigations, both theoretical and experimental, take into account several elements such as: transformer specification, thermal characteristics of the materials involved, transformer construction aspects; as well as the data collected in the experimental measurement, including the temperature at several points of the transformer, applied power and ambient temperature.

So, it is possible to perform of dry-type power transformer simulations to estimate its temperatures at various points and obtain thermal images of the variation and distribution of temperature that occurs internally and externally to the equipment. In this way, the data collected in the experimental measurement can be compared with the results obtained in simulations.

## II. BACKGROUND

Some analytical and experimental studies of the temperature distribution in some types of dry-type transformers have been presented in the literature.

To this end a thermal mathematical model that calculates of the hottest spot temperature and its location in dry-type transformer windings was performed by [6].

This approach was based on three mechanisms of heat transfer: conduction, convection and radiation. However, the finite difference method was applied, and circular or oval forms of transformer geometry suggested finite element analysis to improve numerical accuracy. The heat conduction equation was also solved by the finite difference method by [7] in order to obtain the temperature distribution for the dry-type transformer at steady state.

The two-dimensional (2D) temperature distribution was calculated in [8] using finite element analysis, addressed by CFD (Computational Fluid Dynamics) analysis and using commercial ANSYS software. This work did not consider heat dissipation by thermal radiation.

Thermal analysis and temperature distribution of the transformers were also performed by [9] using a mathematical model using the finite difference method and cylindrical coordinates. To validate the model, the results were compared with the experimental data measured from an 800kVA transformer.

Another 2D thermal study of the cast-resin dry-type transformer was solved in [10] using cylindrical coordinates and the FEM to obtain temperatures in any location of the transformer. Basic modes of heat transfer, such as conduction, convection, and radiation were also used to obtain the steady-state temperature distribution of the transformer.

More recently, a coupled thermal-electromagnetic model for disc-type and foil-type winding to propose temperature distributions using FEM was performed by [11].

The proposed model was based on mechanisms of heat transfer, i.e. conduction heat, convection and radiation, in addition to some electromagnetic mechanisms. All the cooling surfaces were identified and heat transfer coefficients for each surface were presented. The model was applied to a 2,000kVA dry-type power transformer under different load conditions. Experimental temperatures were measured with thermocouples and infrared thermometers and used to compare the results of finite element simulations. In addition, in this model, commercial COMSOL software was used for 2D thermal modeling [11]. The results of [6]-[11] showed reasonable agreement between the calculated data and the experimental data.

In this sense, the present paper presents a thermal simulation of 500kVA dry-type transformer at steady state, with an approach based on the three mechanisms of heat transfer: conduction, convection and radiation; in cartesian coordinates, using the MEF as numerical method and the FEMM (Finite Element Method

Magnetics) 2D software to perform the thermal simulation.

### III. THERMAL STUDY IN DRY-TYPE TRANSFORMERS

The general equation of heat diffusion in cartesian coordinates 2D and steady state is represented in (1), in which it provides a basic tool for the analysis of heat conduction. From the solution of this equation it is possible obtain the temperature distribution  $T(x, y)$  of a steady-state material [12].

$$\frac{\partial}{\partial x} \left( k_x \frac{\partial T}{\partial x} \right) + \frac{\partial}{\partial y} \left( k_y \frac{\partial T}{\partial y} \right) + \dot{q} = 0 \quad (1)$$

Where  $k_x$  and  $k_y$  are the thermal conductivity [W/(m.K)] in the directions of  $x$  and  $y$ ,  $\dot{q}$  is the heat generation by volume [W/m<sup>3</sup>] and  $T$  is the temperature [K].

According to [13], the term heat generation ( $\dot{q}$ ) is defined in (2) as the amount of thermal energy that is generated per unit volume, which in turn is determined by the amount of power loss in a unit volume.

$$\dot{q} = \frac{\dot{E}_{ger}}{V} = \frac{I^2 R}{V} \quad (2)$$

Where  $\dot{E}_{ger}$  is the total rate of heat generation [W],  $I$  is the electric current [A],  $R$  is the electric resistance [ $\Omega$ ], and  $V$  is the conductor volume [m<sup>3</sup>].

The total rate of heat generation is a function of the amount of current flow in a conductor and the resistance of said conductor.

The conductor resistance is calculated according to (3).

$$R = \frac{\rho_e \cdot l}{A_c} \quad (3)$$

Where  $\rho_e$  is the electrical resistivity [ $\Omega \cdot m$ ],  $l$  is the mean conductor length [m] and  $A_c$  is the conductor area [m<sup>2</sup>].

#### 3.1 Boundary Conditions

When no boundary conditions are explicitly defined, each boundary imposes an isolated condition. However, a non-derived boundary condition must be defined somewhere (or the potential must be defined at a reference point in the domain) so that the problem has a unique solution [14]. The convection (4) and radiation (5) equations were used as boundary conditions of (1).

$$k \frac{\partial T}{\partial n} + h(T - T_0) = 0 \quad (4)$$

$$k \frac{\partial T}{\partial n} + \varepsilon \sigma (T^4 - T_0^4) = 0 \quad (5)$$

Where  $h$  is the convective heat transfer coefficient [W/(m<sup>2</sup>.K)],  $T_0$  is the ambient temperature [K],  $\varepsilon$  is the emissivity of the surface,  $\sigma$  is the Stefan-Boltzmann constant [W/(m<sup>2</sup>.K<sup>4</sup>)] and  $n$  represents the direction normal to the boundary.

#### IV. EXPERIMENTAL MEASURES

The transformer used for the experimental measurements was 500kVA from the company Comtrafo, which has a transformation ratio of 13.8kV to 220/127V, and it is in full use on the Sao Bernardo do Campo campus of the Federal University of ABC, as illustrated in Fig. 1.



Fig. 1. Dry-type transformer used for the experimental measurements. Source: Authors.

The equipment used for temperature measurements was a thermal imager, also known as a thermal imaging camera and a temperature sensor of type PT100 installed in the low voltage winding of the transformer.

A three-phase power analyzer was used to measure electrical quantities, such as: voltage, current and power. The quantities were collected at the same time that the temperature data was measured.

Fig. 2 illustrates some of the equipment used in the experimental measurements.

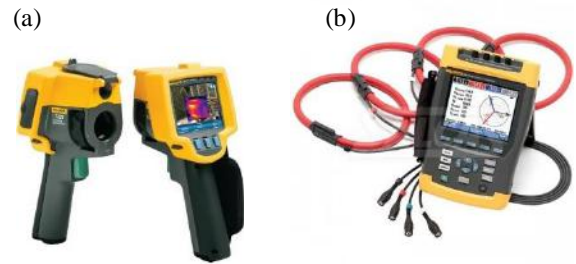


Fig. 2. Equipment used for the reading of temperature (a) and electrical quantities (b). Source: Fluke [15].

For the interpretation and treatment of the collected data, the specific software analyzer was used.

Since the thermal behavior is analogous in the three phases (coils) of the transformer, both the measurements and the simulations were performed in only one of the phases.

Fig. 3a [16] illustrates the details of one of the transformer phases used for collecting measurements and Fig. 3b shows the thermal variation found on the external surface using the thermal imager.

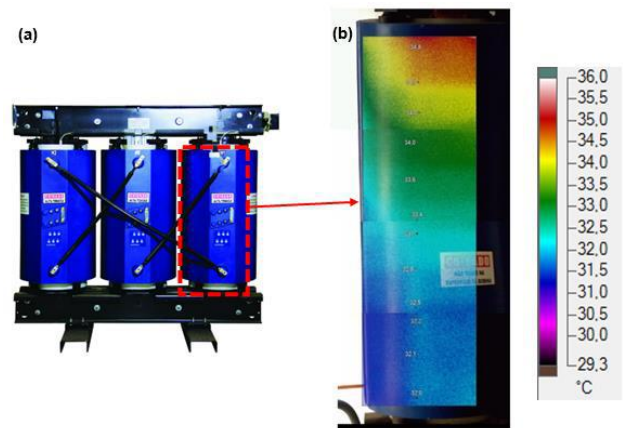


Fig. 3. Detail of one of the phases of the transformer used for measurement (a) and its thermal variation for a given power measured in °C (b). Source: (a) Comtrafo [16], (b) Authors.

Since the thermal imager has a limited visible screen and there were space constraints at the location where the transformer was located, the union of four image segments of the thermal imager was used, all being of the same scale, thus forming a single image of thermal variation on the surface transformer, as shown in Fig. 3b.

TABLE 1 shows the data collected from the electrical energy analyzer, for four different charging situations (powers).

Table.1: Data collected from the energy analyzer for different loading potences.

Reading	Voltage [V]	Current [A]	Power [W]
1	128.8	63.66	8,200
2	128.4	74.83	9,608
3	128.7	97.44	12,540
4	128.5	130.82	16,810

Source: Authors.

TABLE 2 shows the temperature results collected from the thermal imager and the thermal sensor considering the four different loading powers of TABLE 1.

Table.2: Data collected from temperature meters for different loading potences.

Reading	Ambient Temp. [°C]	Thermal Imager [°C]		Thermal Sensor [°C]
		Lower	Upper	

1	23	31.3	33.8	50.3
2	27	31.7	34.5	50.6
3	31	32.0	34.8	50.7
4	28	31.8	34.9	50.8

Source: Authors.

### V. COMPUTATIONAL SIMULATION

As a pre-processing stage and for the realization of the 2D design of the transformer in the FEMM software, the constructive characteristics provided by the manufacturer and the constant dimensions proposed in [9] were used.

The creation of core geometry and low and high voltage windings (LV and HV) were performed only in one of the phases of the transformer.

Considering the symmetry of the sides of the coil and to reduce the speed of the system solution process, the simulation was performed in only one side of the coil, as illustrated in Fig. 4.

The data of the thermal characteristics of the materials used in the core, low/high voltage windings and in the insulation material, such as: M4 silicon steel, aluminum alloy 1,350 and epoxy resin, respectively, and their variations of thermal conductivity in relation to the increase in temperature were also provided by the manufacturer. These thermal characteristics of the materials used and the ambient air were considered in the simulations.

As boundary conditions, the variables used in solving the Equation (4) were: convective coefficients and ambient temperature. For the resolution of (5) the

variables involved were: emissivity and ambient temperature.

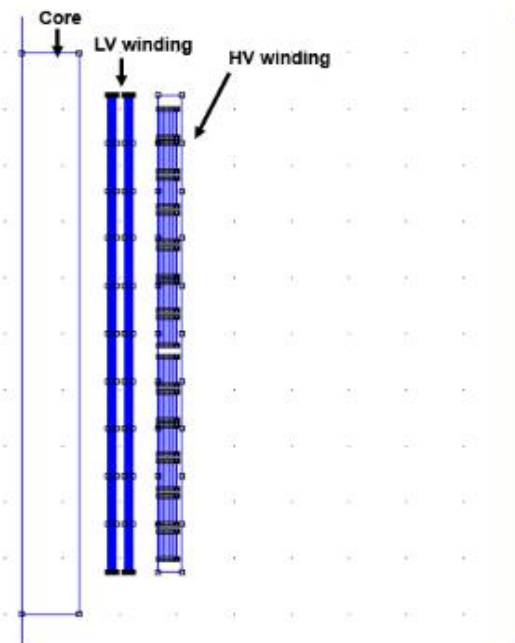


Fig. 4. 2D drawing of one side of the transformer coil in the FEMM software. Source: Authors.

In order to meet the required variables in (4), the surface where convective heat transfer occurs was identified and divided into sections along the height, these partitions being uniform throughout the low and high voltage winding. The values of the upper and bottom convective coefficients of [11] were used as reference for the simulation. The convective coefficients of the interval between the upper and bottom limits were calculated based on the temperature difference and the number of sections considered.

In (5), for the emissivity values, the data of [13] was used as reference and approximation of the values. The emissivity values are based on the temperature of 300K. The values of the ambient temperatures for both (4) and (5) were presented in TABLE 2.

The calculated values of the total rate of heat generation [W] were also considered in the FEMM software. These values are calculated according to (2), in which they vary with current and electrical resistance. The electric current ( $I$ ) was collected directly in the transformer through the electric energy analyzer, as verified in TABLE 1. The equation (3) was used to calculate the resistance of the conductor.

To finalize the pre-processing, the computational domain was adapted and the mesh refinement was carried out, which boils down to increasing the minimum allowed angle for small triangles to be created. Thus, the meshes were created, and the domains of the problem were

divided into finite elements using Lagrange triangular elements, which is the FEMM standard element type.

Fig. 5 shows the meshes of all domains, including core and low and high voltage windings.

The processing step consists in solving the problem, based on the parameters and variables defined in the pre-processing. The software performs internally the matrix representation of each element, formation of the global coefficient matrix, application of the boundary conditions and, finally, the solution of the system.

After this, at the final step, post-processing, the graphical and numerical results are presented.

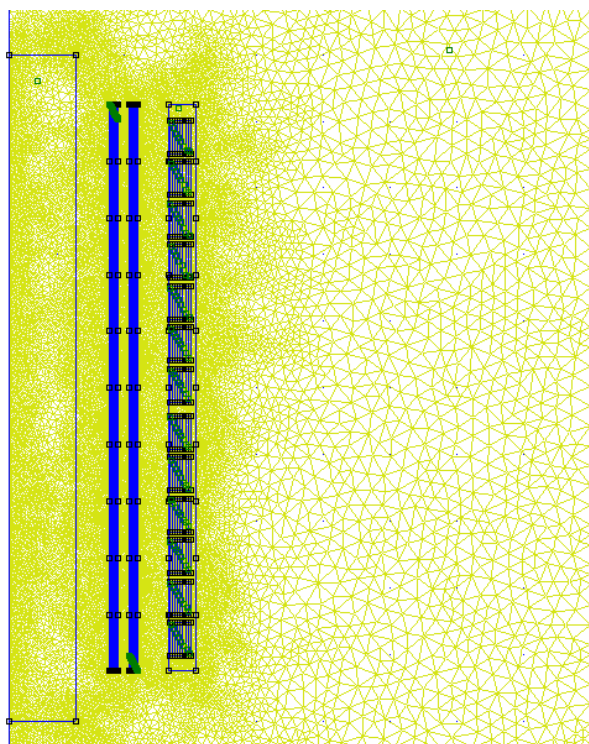


Fig. 5. Finite element domains divided into triangular elements. Source: Authors.

## VI. RESULTS AND DISCUSSIONS

The thermal simulation results obtained in the post-processing step are visualized in Fig. 6.

In the highlighted approach of Fig. 6 it is seen that the temperatures in the upper part are higher than in the bottom part, this is because different convective coefficients were applied in the sections of the windings surfaces, being in agreement with the variations of the values collected in the experimental measurement for high voltage windings.

The temperature data obtained in Fig. 6 are in Kelvin and the TABLE 3 presents the values of the points in °C.

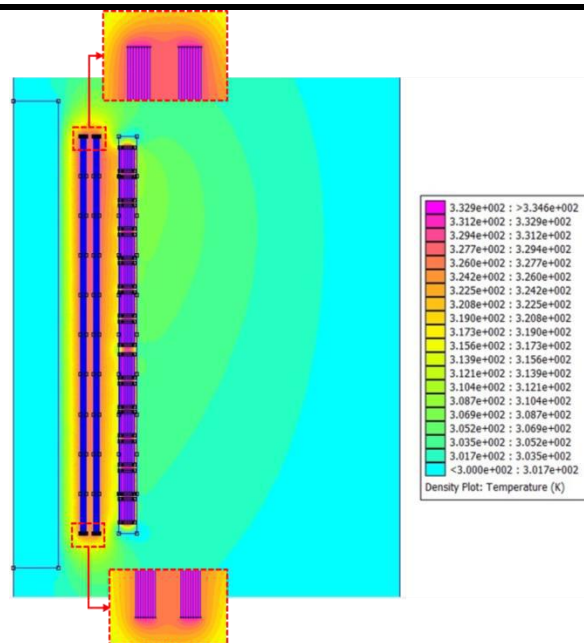


Fig. 6. Visualization of thermal simulation results. Source: Authors.

The TABLE 3 also presents the comparison between the temperatures measured experimentally with the values obtained in the thermal simulation, as well as the absolute and relative error. From TABLE 3 it is possible to observe low absolute and relative errors and that there was a direct relationship of the transformer operating temperature increase when compared to the transformer power increase and the ambient temperature.

Table 3. Comparative of temperature measures and simulated and their respective errors.

Power [W]	Site	Temperature			
		Measured [°C]	Simulated [°C]	Absolute Error [°C]	Relative Error
8,2	Surface				
	HV	31.30	33.75	2.45	8%
	Bottom				
	Surface				
	HV	33.80	36.85	3.05	9%
	Upper				
9,60	LV Winding	50.30	54.90	4.60	9%
	Surface				
	HV	31.70	34.70	3.00	9%
8	Bottom				
	Surface				
	HV	34.50	37.65	3.15	9%
	Upper				

	LV Winding	50.60	54.70	4.10	8%
	Surface				
	HV Bottom	32.00	34.80	2.80	9%
12,5	Surface				
4	HV Upper	34.80	37.85	3.05	9%
	LV Winding	50.70	55.50	4.80	9%
	Surface				
	HV Bottom	31.80	34.50	2.70	8%
16,8	Surface				
1	HV Upper	34.90	37.85	2.95	8%
	LV Winding	50.80	55.60	4.80	9%

Source: Authors.

The Fig. 7 illustrates the data presented in TABLE 3, which shows the measured and simulated temperature variations for the power of 8,200W.

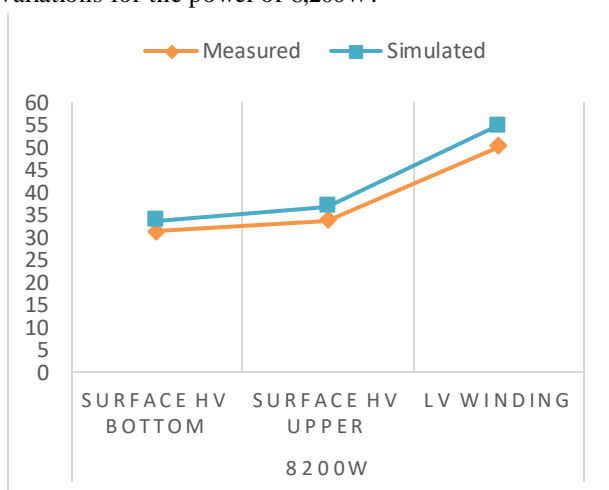


Fig. 7. Measured and simulated temperatures with load power of 8,200W. Source: Authors.

Comparing Fig. 3b, image obtained experimentally, with Fig. 6, simulated image, it is verified that both have a vertical temperature gradient. This characteristic occurs because the convective heat transfer is larger in the bottom part and smaller in the upper part, obtaining higher temperatures on the upper surface and lower on the bottom surface. Further, it becomes apparent that the air temperature is heated with increasing axial length, whereby the natural convection cooling effect is therefore greater in the bottom windings.

It can also be seen in Fig. 7 that the values measured experimentally compared to the simulated values for the

same power also showed agreement on the temperature variation on the surface and on the transformer windings.

### 6.1 Error Analysis

The errors found and described in TABLE 3 may be related to the conditions considered in the thermal simulation or even by inaccuracies in the experimental measurements.

Thus, effects of some factors on the temperature distribution of the measurements collected experimentally and the simulations carried out in FEMM software may have influenced the results, such as: inaccuracies and uncertainties involving the temperature readings by the thermal imager and the sensor, in the experimental part; and errors caused by numerical calculations due to some computational operations, such as rounding and estimation, in the theoretical part. Other prominent factors were:

I. Some measurements of the size / dimensions for the formation of the transformer geometry were approximated, also contributing to the divergence of measured and simulated values;

II. The simulation was performed in the 2D domain and in cartesian coordinates, and the 3D computational domain and cylindrical coordinates could present more accurate values, since they are closer to the actual configurations and geometries of the transformer;

III. Only the thermal study of the transformer was considered, not taking into account the electromagnetic interferences in the winding and the core of the transformer;

IV. The values of the boundary conditions for the convective coefficients and emissivities were also approximated for the geometry and applied materials, respectively;

V. The conductor resistivity variation was not taken into account with increasing winding temperature and ambient temperature, considering that the resistivity, and consequently the resistance, vary with the increase in temperature over time.

## VII. CONCLUSION

In this work it was possible to demonstrate that the finite element analysis provides an efficient tool for determining the temperatures along a dry-type transformer under load. Furthermore, the heat transfer analysis allows to predict the temperature in several locations of the transformer and the temperature distribution considering different operating conditions.

Thus, considering that the transformer was simulated in two-dimensional geometry, with some characteristics and measures of approximate size/dimensions, it has been that the thermal simulation showed agreement with the

temperature variations of the transformer measured experimentally.

Finally, the results of this study may provide manufacturers with a better understanding of the nature of heat transfer in transformers, and may help to deal with thermal stresses more effectively.

#### ACKNOWLEDGEMENTS

We are grateful to the Universidade Federal do ABC (UFABC) for providing the facilities for the corresponding measurements.

#### REFERENCES

- [1] P. K. Sen (2003), "Application guidelines for dry-type distribution power transformers," in *Industrial and Commercial Power Systems*. IEEE Technical Conference.
- [2] J. Smolka, A. J. Nowak (2008), "Experimental validation of the coupled fluid flow, heat transfer and electromagnetic numerical model of the medium-power dry-type electrical transformer," *International Journal of Thermal Sciences* 47, pp. 1393-1410.
- [3] M. K. Pradhan, T. S. Ramu (2003, November), "Prediction of hottest spot temperature (HST) in power and station transformers," *IEEE Trans. Power Delivery*, vol. 18, No. 4, pp. 1275–1283.
- [4] M. Lee, H. A. Abdullah, J. C. Jofriet, and D. Patel (2010, January), "Thermal modeling of disc-type winding for ventilated dry-type transformers," *Electric Power Systems Research*, vol. 80, pp. 121-129.
- [5] M. A. Tsili *et al* (2012), "Power transformer thermal analysis by using an advanced coupled 3D heat transfer and fluid flow FEM model," *International Journal of Thermal Sciences* 53, pp. 188-201.
- [6] L. W. Pierce (1994, April), "Predicting hottest spot temperatures in ventilated dry type transformer windings," *IEEE Trans. Power Delivery*, vol. 9, No. 2, pp. 1160-1172.
- [7] Z. Dianchun, Y. Jiaxiang, W. Zhenghua (2000), "Thermal field and hottest spot of the ventilated dry-type transformer," in *Proceedings of the 6th International Conference on Properties and Applications of Dielectric Materials*, vol. 1, pp. 141–143.
- [8] G. Kömürgöz, Í. Özkol (2003), "Predicting hottest spot temperature in self-cooled dry-type transformer," in *International Conference on Electrical and Electronics Engineering*, ELECO, pp. A2–06.
- [9] E. Rahimpour and D. Azizian (2006, April), "Analysis of temperature distribution in cast-resin dry-type transformers," *Electr. Eng.*, pp. 301-309.
- [10] M. B. Eteiba, E. A. Alzahab, Y. O. Shaker (2010), "Steady state temperature distribution of cast-resin dry type transformer based on new thermal model using finite element method," in *International Journal of Electrical, Computer, Energetic, Electronic and Communication Engineering*, vol. 4, No. 2.
- [11] M. Lee *et al* (2010, September), "Temperature distribution in foil winding for ventilated dry-type power transformers," *Electric Power Systems Research*, vol. 80, pp. 1065-1073.
- [12] F. P. Incropera *et al* (2008), "Fundamentos de Transferência de calor e de massa," 6th ed., Rio de Janeiro: LTC.
- [13] Y. A. Çengel, A. J. Ghajar (2012), "Transferência de calor e massa: uma abordagem prática," 4th ed., Porto Alegre: McGraw-Hill.
- [14] D. Meeker. (2015, October). Finite Element Method Magnetics - User's Manual. Version 4.2. 2015. [Online]. Available: <http://www.femm.info/Archive/s/doc/manual42.pdf>.
- [15] Fluke Products. (2017, April), [Online]. Available: <http://en-us.fluke.com/products/all-products/>.
- [16] Comtrafo Industria de Transformadores Elétricos S.A. (2017, April), Transformadores a Seco. [Online]. Available: <https://www.comtrafo.company/transformador-a-seco>.